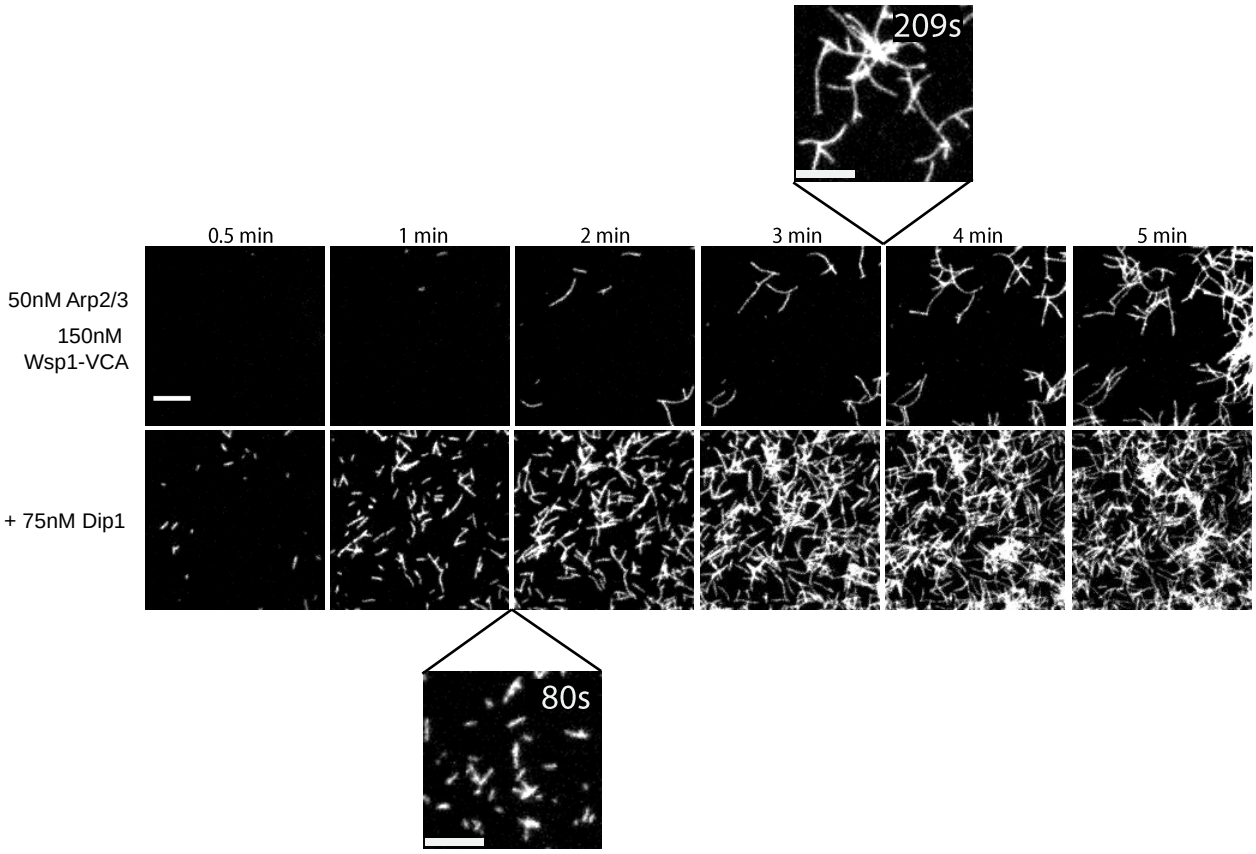

Figure S1: Visualization of TIRF images for reactions with or without Dip1 at equivalent timepoints. Related to Figure 1. Actin polymerization assays contained 150 nM GST-Wsp1-VCA, 1.5 µM 33% Oregon Green-labeled actin and 50 nM SpArp2/3 complex in the presence or absence of 75 nM Dip1. The reaction time is indicated above each pair of images. Frames used for quantification from Figure 1A are shown above or below the corresponding time series. Because polymer accumulates rapidly to fill the field of view in the presence of Dip1, we could not compare branching densities for reactions with or without Dip1 at identical timepoints. Scale Bars: 5 µm.

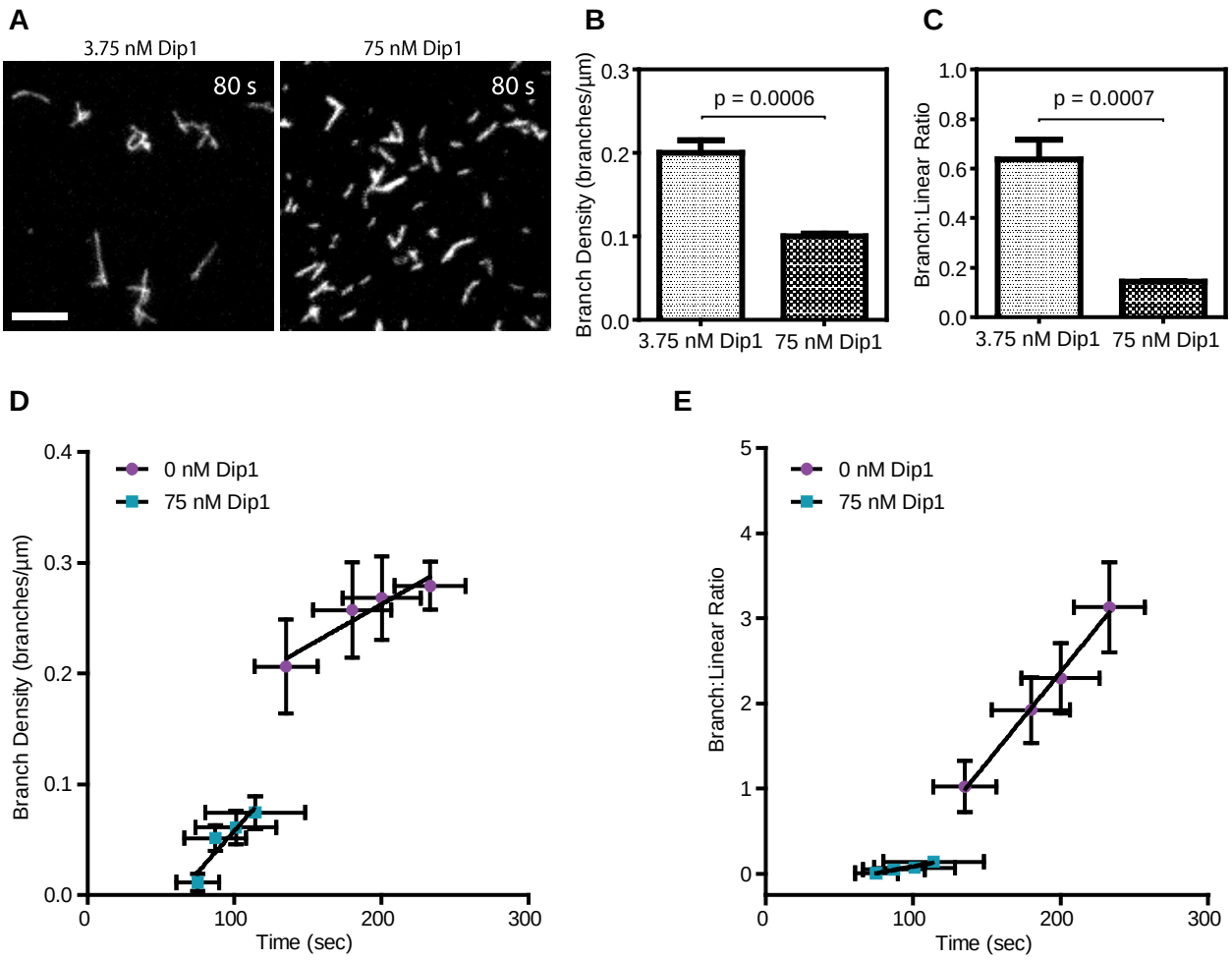

Figure S2: Dip1 decreases branching density and branch to linear filament ratio in reactions containing Wsp1. Related to Figure 1. A. TIRF images showing reactions containing 150 nM GST-Wsp1-VCA, 1.5 µM 33% Oregon Green-labeled actin, 50 nM SpArp2/3 complex and either 3.75 nM or 75 nM Dip1, 80 seconds after initiating the reaction. Scale bar: 5 µm. **B.** Bar plot showing the branch density of actin filaments in TIRF reactions in panel A. **C.** Bar plot comparing the ratio of the total number of branches to the total number of actin seed filaments in the same reactions as in panel B. Error Bars for panel B and C: SE from 4 regions of interest containing at least 45 µm of total actin filaments from a single reaction for each condition. The reported p-values are the result of two-tailed t-tests assuming unequal variances. **D.** Plot showing the branch density over time in reactions containing 150 nM GST-Wsp1-VCA, 1.5 µM 33% Oregon Green-labeled actin and 50 nM SpArp2/3 complex with or without 75 nM Dip1. The four plotted time points for each condition represent the average time at which the reactions hit 250, 500, 750 and 1500 µm of total actin filament. The best fit line for each condition is plotted over the data. **E.** Plot showing the ratio of the total number of branches to linear filaments in the same reactions as in panel D. Error Bars for panel D and E: y-axis; SE from 4 regions of interest from 2 reactions for each condition, x-axis; SE of the average times for the equivalent reactions for each condition to reach the total actin filament lengths reported for panel D.

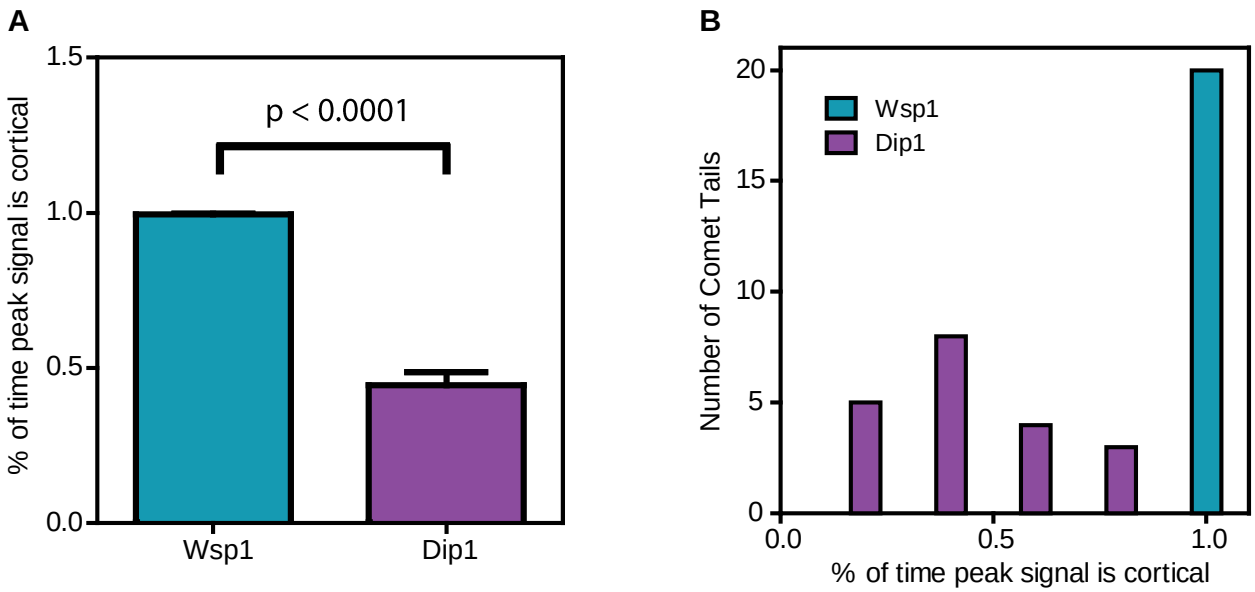

Figure S3: Wsp1 remains predominantly cortical, while Dip1 often moves inward with treadmilling actin comet tails. Related to Figure 3. A. Bar plot showing the percentage of time (# of frames) that the peak signal of Dip1-mNeonGreen and GFP-Wsp1 is cortical. Error Bars: SE from 20 comet tails measured from 6 or 8 cells for Wsp1 and Dip1, respectively. The reported p-value is the result of a two tailed t-test assuming unequal variances. **B.** Histogram of the data from panel A showing the number of comet tails in which Dip1-mNeonGreen or GFP-Wsp1 was cortical for the specified percentage of the lifetime of the comet tail.

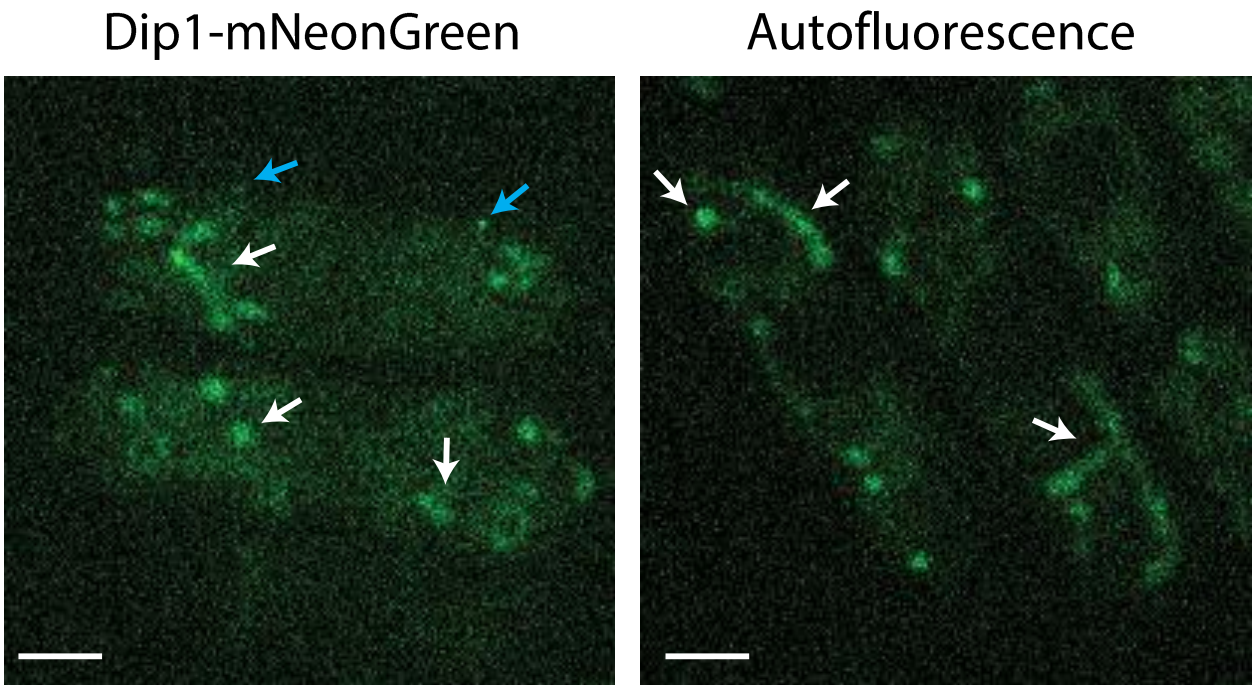

Figure S4: Under conditions required to visualize Dip1-mNeonGreen, autofluorescent structures were observed in some cells. Related to Figure 3. Spinning disk microscope image of *S. pombe* cells expressing mCherry-Wsp1 and Dip1-mNeonGreen (left) or unlabeled Dip1 (right) after 15 seconds of 300 ms exposures of 25 mW 488 laser at 1 second intervals. White arrows point out examples of large autofluorescent structures present after passing through a 525 nm (50 nm bandwidth) emission filter, even in the absence of an mNeonGreen label. The Dip1 signal is distinguishable from the autofluorescent structures because it is dynamic, small, punctate and partially colocalizes with Wsp1 (VideoS2). Blue arrows show examples of Dip1-mNeonGreen signal at endocytic sites. Scale Bar: 2 µm.